of rapid filtration [E. Prossnitz, A. Gee, G. F. Ames, *J. Biol. Chem.* **264**, 5006 (1989)] and was calculated according to Robertson *et al.* [D. E. Robertson, G. J. Kaczorowski, M. L. Garcia, H. R. Kaback, *Biochemistry* **19**, 5692 (1980)]. No energy sources other than light were added to the vesicles, and the experiments were conducted at room temperature.
21. R. A. Bogomolni *et al.*, *Proc. Natl. Acad. Sci. U.S.A.* **91**, 10188 (1994).
22. V. J. Yao and J. L. Spudich, *Proc. Natl. Acad. Sci. U.S.A.* **89**, 11915 (1992).
23. R. Seidel *et al.*, *Proc. Natl. Acad. Sci. U.S.A.* **92**, 3036 (1995).
24. N. R. Pace, *Science* **276**, 734 (1997).
25. J. A. Fuhrman, K. McCallum, A. A. Davis, *Appl. Environ. Microbiol.* **59**, 1294 (1993).
26. T. M. Schmidt, E. F. DeLong, N. R. Pace, *J. Bacteriol.* **173**, 4371 (1991).
27. M. T. Suzuki *et al.*, *Appl. Environ. Microbiol.* **63**, 983 (1997).
28. M. S. Rappe, P. F. Kemp, S. J. Giovannoni, *Limnol. Oceanogr.* **42**, 811 (1997).
29. S. G. Acinas, J. Anton, F. Rodriguez-Valera, *Appl. Environ. Microbiol.* **65**, 514 (1999).
30. M. T. Suzuki *et al.*, unpublished data.
31. H. Eilers, J. Pernthaler, F. O. Glockner, R. Amann, *Appl. Environ. Microbiol.* **66**, 3044 (2000).
32. J. G. Keunen, L. A. Robertson, O. H. Tuovinen, in *The Prokaryotes*, A. Balows, H. G. Truper, M. Dworkin, W. Harder, K. H. Schleifer, Eds. (Springer, Berlin, 1991), pp. 2638–2657.
33. Single-letter abbreviations for the amino acid residues are as follows: A, Ala; C, Cys; D, Asp; E, Glu; F, Phe; G, Gly; H, His; I, Ile; K, Lys; L, Leu; M, Met; N, Asn; P, Pro; Q, Gln; R, Arg; S, Ser; T, Thr; V, Val; W, Trp; and Y, Tyr.
34. J. Sasaki and J. L. Spudich, *Biophys. J.* **75**, 2435 (1998).
35. We thank C. M. Sakamoto for help with pH measurements and the captain and crew of the RV *Point Lobos* for sampling opportunities at sea. This work was supported in part by NSF grant OCE 0001619 (E.F.D.), by support provided to the Monterey Bay Aquarium Research Institute by the David and Lucile Packard Foundation, by NIH grants HG01775-02S1 (S.B.J.) and R01GM27750 (J.L.S.), and by a long-term postdoctoral fellowship to O.B. from the European Molecular Biology Organization.

9 May 2000; accepted 7 August 2000

REPORTS

Optically Induced Entanglement of Excitons in a Single Quantum Dot

Gang Chen,[1] N. H. Bonadeo,[1]* D. G. Steel,[1]† D. Gammon,[2] D. S. Katzer,[2] D. Park,[2] L. J. Sham[3]

Optically induced entanglement is identified by the spectrum of the phase-sensitive homodyne-detected coherent nonlinear optical response in a single gallium arsenide quantum dot. The electron-hole entanglement involves two magneto-excitonic states differing in transition energy and polarization. The strong coupling needed for entanglement is provided through the Coulomb interaction involving the electrons and holes. The result presents a first step toward the optical realization of quantum logic operations using two or more quantum dots.

Entanglement is one of the most spectacular peculiarities of quantum mechanics that contrast with classical physics (*1*). While it can occur between separate degrees of freedom of a single particle (*2*), only interparticle entanglement bears the properties of nonlocality that are essential for quantum information manipulation (*3*), such as teleportation, cryptography, and computation (*4*). Entangled states involving photons (*5*) or massive particles (*6–9*) have been produced by various experimental means. In addition, fundamental quantum logic gates and a number of quantum algorithms have also been demonstrated using these systems (*10–12*).

Recently, semiconductor quantum dot (QD) systems have been proposed as the basic building blocks for solid-state–based quantum logic devices due to their potential advantages, including the existence of an industrial base for semiconductor processing and the ease of integration with existing devices (*13–15*). The rapid technological advances seem to promise sophisticated engineering of the QD structures with the potential for the production of scalable coupled-QD systems (*16, 17*). However, neither entanglement nor any quantum logic operation has been realized in these systems.

We report the production and detection of an entangled state involving two excitonic states localized in a single GaAs QD, demonstrating an important first step toward the goal of entangling excitons confined to two or more semiconductor QDs. Single-QD exciton states are addressed with high spatial resolution using optical excitations that promote electrons from the heavy-hole levels of a single QD (with projected angular momentum of $\pm 3\hbar/2$) to the first excited electronic states (with projected angular momentum of $\pm\hbar/2$). An external static magnetic field is applied in the Faraday configuration to split both the hole and electron levels. It has been shown (*18*) that, despite the interacting electron nature of the semiconductor ground state, the low-lying state of a single electron and hole excitation is a well-defined single-particle state and that the exciton is a well-defined electron-hole pair state with only mutual attraction. All relevant energy levels and the two optically allowed circularly polarized (σ_+ and σ_-) transitions at frequencies ω_+ and ω_- are shown (Fig. 1A). Two mutually coherent laser fields, σ_+ polarized at frequency Ω_+ and σ_- at frequency Ω_-, respectively, excite these two transitions, producing the entangled state (Fig. 1B). In the excitonic picture, the total wavefunction can be written as

$$|\Psi\rangle = C_0|0\rangle + C_+|-1/2, +3/2\rangle + C_-|+1/2, -3/2\rangle \quad (1)$$

a nonfactorizable wavefunction involving the $|-1/2, +3/2\rangle$ and $|+1/2, -3/2\rangle$ excitons. Our notation for single-exciton states keeps track of the angular momentum of the excited electron and the hole left behind. The state $|0\rangle$ is the many-exciton vacuum (crystal ground state), $|-1/2, +3/2\rangle$ represents the σ_+ (or spin-up) exciton state where an electron in the $-3\hbar/2$ level is promoted to the $-\hbar/2$ level (through a σ_+ transition), leaving a hole with angular momentum of $+3\hbar/2$. Similarly, $|+1/2, -3/2\rangle$ represents the σ_- (or spin-down) exciton state.

In order to optically excite a nonfactorizable wavefunction and produce an entangled state of two quantum systems, it is known that a strong coupling is required (*19*). In the case of two excitons in a quantum dot, the coupling is due to the strong Coulomb interaction (*20*). This is best seen from the four-level diagram (Fig. 1C) in the two-exciton basis (*21*). While leaving the exciton vacuum and the single-exciton states unaffected, it leads to an energy shift of the two-exciton level $|-1/2, +3/2, +1/2, -3/2\rangle$ (represented by t in the absence of this interaction), which becomes either a bound biexciton state (denoted by b) or a scattering state of two excitons (denoted by s). The photoluminescence of the biexciton state for similar dots in this study have been reported in (*22*). Because of the narrow-band excitation used to excite the single-exciton states, the b (or s) state is out of resonance and therefore does not contribute to

[1]Harrison M. Randall Laboratory of Physics, University of Michigan, Ann Arbor, MI 48109–1120, USA. [2]The Naval Research Laboratory, Washington, DC 20375, USA. [3]Department of Physics, University of California San Diego, La Jolla, CA 92093–0319, USA.

*Present address: Bell Laboratories, 101 Crawfords Corner Road, Holmdel, NJ 07733, USA.
†To whom correspondence should be addressed. E-mail: dst@eecs.umich.edu

the total wavefunction in Eq. 1. This situation is analogous to the case of producing entangled states of trapped ions (*23*). Without exciton-exciton interactions, however, level t would contribute an extra term $C_t|-1/2, +3/2, +1/2, -3/2\rangle$ in Eq. 1 with an appropriate probability amplitude ($C_t = C_-C_+/C_0$) to produce a factorizable wavefunction.

For our measurements, we use a coherent nonlinear optical (CNO) spectroscopy technique that involves two continuous-wave laser fields arranged in the pump-and-probe geometry (*24, 25*). The resulting signal field produced by the CNO interaction is homodyne-detected with the transmitted probe beam. In the weak-field limit, the signal is proportional to the imaginary part of the third-order susceptibility $\chi^{(3)}$ [or polarization $P^{(3)}$] of the system. The excitation beams, frequency stabilized to 4 neV, are independently and continuously tunable, allowing us to explore the QD system in two ways. The CNO response of the magneto-excitons is first studied using the degenerate response ($\Omega_{pump} = \Omega_{probe}$). To detect the exciton entanglement, we use the nondegenerate configuration, where the pump-and-probe fields are tuned to excite different excitonic transitions.

The QDs used in our experiments are naturally formed by interface fluctuations in a 42 Å GaAs quantum well (with 250 Å $Al_{0.3}Ga_{0.7}As$ barriers) with growth interruptions and are probed through submicrometer-sized apertures (*26, 27*). The heavy-hole excitons localized in these QDs show extremely narrow photoluminescence (PL) lines and an atomic-like PL excitation spectrum (*27*). The CNO response is dominated by Pauli blocking of electrons (*24*) with insignificant pure dephasing. Excitation-induced dephasing or other many-body effects has not been observed in these systems, in sharp contrast with higher dimensional semiconductor structures. Due to the asymmetry of the interface island elongation that leads to band mixing, the optically allowed doublet follows linearly polarized selection rules in the absence of an applied magnetic field, and shows a small fine structure splitting (*26*). An external magnetic field, in addition to splitting all electronic levels, diminishes the exchange interaction that causes band mixing, recovering the circular polarization of the optical transitions (*28*).

The spectrum of a fully degenerate CNO experiment is shown (Fig. 2A) at zero magnetic field using co-linearly polarized pump and probe, with sharp spectral peaks arising from single QD excitons, similar to that first reported in (*24*). The degenerate CNO response of a typical QD as a function of the magnetic field is shown (Fig. 2B). The polarization of both the excitation beams are σ_+ (or σ_-), so that they jointly excite and map out the corresponding exciton resonance without providing information about exciton-exciton coupling. It shows that the magnetic field recovers the circular polarization selection rules of the exciton transitions and results in a Zeeman splitting and a diamagnetic shift of the resonances. The two excitons are not mixed and are both energetically and orientationally differentiable under even a small magnetic field, implying that exchange effects are negligible. The nonlinearity caused by the Overhauser effect (*28*) is efficiently suppressed by fast modulation of the beams. Note that both the linewidth and the signal strength of the σ_+ and the σ_- transitions are comparable within experimental error (±5%), showing an identical dipole moment (or oscillator strength) and dephasing rate, as expected.

To entangle the two magneto-excitonic states and detect the entanglement, we tune the σ_- polarized "pump" field to excite the lower energy transition, and measure the CNO spectrum as the σ_+ polarized "probe" field excites the higher energy excitonic transition (compared to the experiment where the higher energy exciton state is "pumped" and the lower energy one is "probed," this configuration avoids the contribution from the incoherent spin-flip of the higher energy exciton). As the theory presented below will show, a unique interference lineshape seen in the spectrum identifies a second-order (in the applied optical fields) coherence between the two excitonic states induced by the presence of both optical fields. This coherence implies a well-defined phase relation between C_+ and C_- of Eq. 1, from which we infer the presence of quantum entanglement between the two excitonic states.

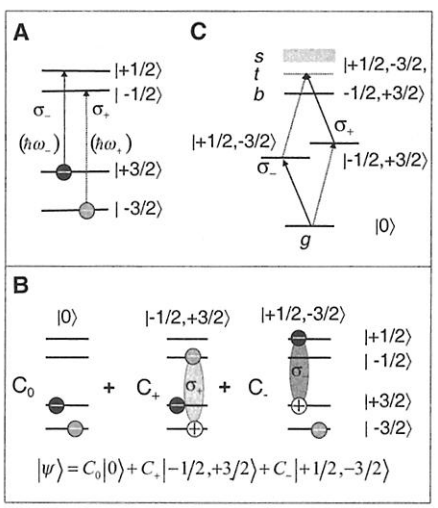

Fig. 1. (**A**) Level diagram for heavy-hole exciton transitions of a GaAs quantum dot under an external magnetic field. (**B**) The entanglement implied by a nonfactorizable wavefunction involving the σ_- and the σ_+ excitons. (**C**) The four-level model for incorporating the Coulomb correlation into the problem. The noninteracting two-exciton, bound biexciton, and scattering states of two excitons are represented by t, b, and s, respectively. σ_+ and σ_- represent the two single-exciton states and g the exciton vacuum (crystal ground state).

In the absence of the Coulomb interaction, the two excitonic transitions would be independent of each other. In this case, not only is there no entanglement, there is also no nonlinear signal, because the excitation of the σ_- exciton (by the σ_- polarized pump beam) would not affect the σ_+ excitonic transition, to which the σ_+ polarized probe beam is sensitive. The exciton-exciton Coulomb interaction, however, causes only an energy shift of the two-exciton level (Fig. 1C). Under the condition that both beams are well off-resonance with the energy-shifted state, the problem is effectively reduced to three levels. This gives rise to a nonzero nonlinear signal, which allows for the study of the coherent coupling between the σ_+ and σ_- excitons. Any contribution from the two-exciton level would lead to reduction of signal strength. As will be shown later, we observe no such reduction. Therefore, the total excitonic state of the system after excitation is a coherent superposition as shown in Eq. 1.

To explain the nondegenerate CNO experiment, the third-order polarization of the experiment (polarization of the σ_+ exciton) is calculated under steady-state conditions using the density matrix formalism for a three-level system in the rotating wave approximation (*29*)

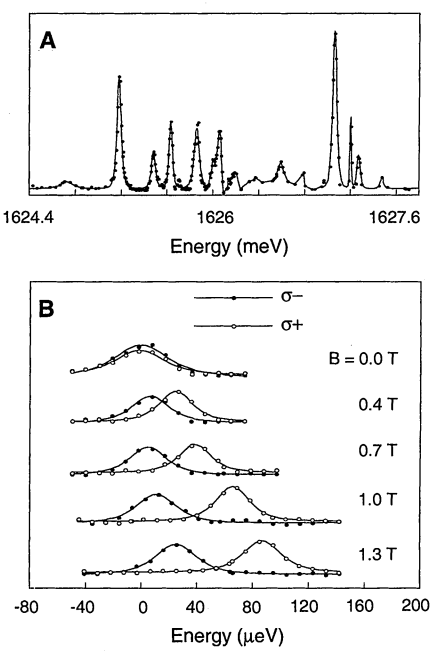

Fig. 2. (**A**) High-resolution degenerate ($\Omega_{pump} = \Omega_{probe}$) coherent nonlinear measurement through a 0.5-mm aperture showing sharp spectral lines from single GaAs QDs at 0 B-field and T = 5 K. The pump and probe beams are co-linearly polarized. (**B**) Field dependence of the degenerate nonlinear response of a typical dot, showing a diamagnetic shift and Zeeman splitting. Solid and open circles correspond to the experimental data where both the pump and probe beam are σ_- and σ_+ polarized, respectively. The horizontal axis denotes the energy detuning from that of the signal peak at zero field.

$$P^{(3)}_{NL} = \frac{-i|\mu_-\mu_+|^2 e^{-(k_{probe}r-\omega_{probe}t)}}{8\hbar^3(\gamma_{31} + i\Delta_{probe})} \left\{ \frac{|E_-|^2E_+}{\Gamma}\left[\frac{1}{\gamma_{21} - i\Delta_{pump}} + \frac{1}{\gamma_{21} + i\Delta_{pump}}\right] + \frac{(E^*_-E_+)E_-}{\gamma_{32} + i(\Delta_{probe} - \Delta_{pump})}\left[\frac{1}{\gamma_{21} - i\Delta_{pump}} + \frac{1}{\gamma_{31} + i\Delta_{probe}}\right]\right\} + c.c \quad (2)$$

where $\Delta_{pump} = \Omega_- - \omega_-$, $\Delta_{probe} = \Omega_+ - \omega_+$. The variable γ_{ij} represents the dephasing rate between level i and j, with level 1, 2, and 3 being the ground, σ_-, and σ_+ states, respectively. Γ is the energy relaxation rate of the σ_- state. The values μ_+ and μ_- represent the dipole of the σ_+ and σ_- transitions, respectively. The pump field is denoted by E_-, whereas the probe field is denoted by E_+.

Equation 2 shows two contributions to the nonlinear signal resulting from different time ordering in perturbation theory. The first term is sometimes referred to as the incoherent contribution and arises from reduced absorption of the σ_+ polarized probe beam following excitation by the σ_- polarized pump [the σ_- field reduces the total population of the ground state in the second-order ($E_-E^*_-$) through the σ_- transition]. It is incoherent since the phase information of the pump is lost in $E_-E^*_-$. This contribution requires no mutual coherence between the fields. The second term of Eq. 2 comes from the coherent coupling between E_+ and E_- leading to a coherence between the σ_+ and σ_- excitons. It is created by $E^*_-E_+$ to the second order; a mutual coherence between E_- and E_+ is essential (*30*).

Figure 3 shows this theoretical prediction of the contribution from each term as well as the total signal, with the pump frequency tuned to different positions around the σ_- resonance. It can be seen that the incoherent contribution peaks at the center of σ_+ resonance, independent of the pump position, indicating its incoherent nature. Interestingly, the inclusion of the coherent contribution introduces a dramatic and qualitative change in the lineshape, and is characterized by the development of an asymmetry due to interference between the two terms and the tracking of the signal peak with the pump position. The presence of the interference lineshape indicates that the coherence between C_+ and C_- is not destroyed by dephasing (decoherence). The sign of the signal is quite distinct from that recently reported in (*31*).

The experimental results are shown in Fig. 4. The results shown are independent of the excitation intensity and are confirmed to be in the $\chi^{(3)}$ regime. The nonzero "cross-polarized" response, which is characterized by an interference lineshape similar to that predicted by theory, provides the following important information: (i) The two excitons are not independent and are coupled through the Coulomb interaction, whose main effect is to shift the two-exciton level. (ii) It is possible to control the spin-up exciton using the spin-down exciton, and vice versa. (iii) The two-exciton coherence is induced in the second order and detected in the third order (in the applied optical fields), implying that the excited wavefunction is indeed a coherent superposition of states as described by Eq. 1. (iv) This coherence is not destroyed in the time scale short compared to the C_+ and C_- lifetime.

The signal strength of both the degenerate and nondegenerate response is used to validate the assumption that the two-exciton level does not contribute to our experiment. Any such contribution would give rise to a reduction in nondegenerate signal strength. Full cancellation of the signal would take place in the noninteracting case, where the two-exciton level would contribute with a probability amplitude $C_t = C_-C_+/C_0$. By comparison with theory, when Eq. 2 is modified to include the fourth level, the data then shows that the reduction is indeed negligible within an experimental error of 5%, which means that the two-exciton level contributes less than $C_t = 5\% \times C_-C_+/C_0$. From the detected signal strength, we are able to obtain $|C_+| = 0.3 \pm 0.05$ and $|C_-| = 0.3 \pm 0.05$. The two-exciton level probability amplitude, $|C_t|$, is less than 0.005 (0.1 would make the total wavefunction factorizable). The value of $|C_0|$ is 0.9. The density matrix for the two-exciton system is then established, from which the entropy of entanglement (*32*), E, is calculated to be $E = 0.08 \pm 0.02$, indicating quantum entanglement. This number is relatively small compared to what has been achieved in an ion trap (*6*) (where an E value of 0.5 is reported) and reflects the weak-field condition of our experiment to stay in the $\chi^{(3)}$ regime, as appropriate for spectroscopy studies where Eq. 2 is valid. For entanglement with $C_0 = 0$ and the eventual application to a quantum logic device, the experiments would be done using high-intensity coherent transient excitations with a pulse area of order π.

The nondegenerate response of Fig. 4 is fully resonant, in the sense that, if either beam is detuned outside the corresponding transition line, the signal vanishes. In addition, if we change the polarization of either or both beams to oppositely circularly polarized (compared to that used in Fig. 4), no signal is observable. These are in contrast with the measurements performed in quantum wells by Sieh and coworkers (*31*), who showed a red-shift type of dispersive lineshape attributed to the presence of two-exciton states. In our experiment, however, the two-exciton state does not play a role. Indeed, if the spectra shown in Fig. 4 were to be attributed to a simple lineshift, it would be a blue shift, instead of a red shift, as is the case in (*31*) under similar experimental conditions.

The coherence we describe resembles the so-called Zeeman coherence in atomic systems.

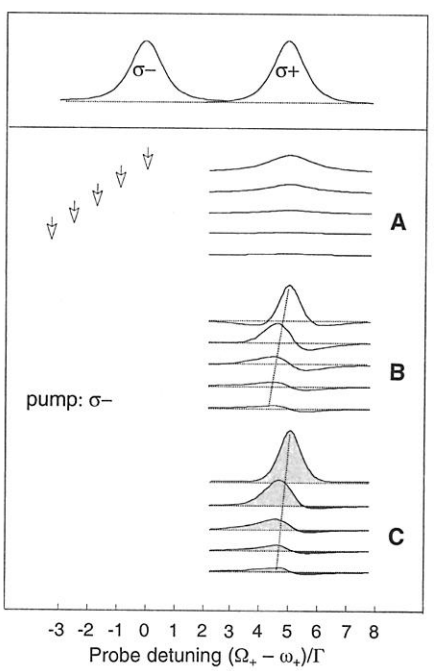

Fig. 3. Theoretical prediction for the nondegenerate experiments with the exciton-exciton Coulomb interaction considered. The pump is σ_- polarized and fixed at positions indicated by the arrows. The probe is σ_+ polarized and scanned across the σ_+ resonance. Curves in (**A**) show the incoherent contribution from the ground-state depletion. Curves in (**B**) show coherent contribution. Curves in (**C**) show the total signal. Without the Coulomb interaction, the nonlinear signal is zero.

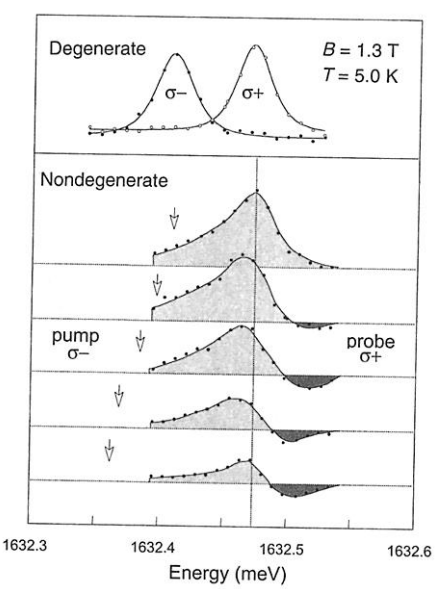

Fig. 4. Nondegenerate coherent nonlinear response of a single QD. The pump is placed at the σ_- (lower) state with σ_- polarization. The probe is scanned across the σ_+ state (upper) with σ_+ polarization. The results show an interference lineshape identifying the contribution from the Zeeman coherence, implying an quantum entanglement of excitons.

Similar coherence between heavy-hole and light-hole excitons has been reported in (*33*). These are examples of quantum coherence involving a nonradiative superposition of states, which leads to many novel phenomena such as the Hanle effect, dark states, lasing without inversion, electromagnetically induced transparency, and population trapping [see (*33*) and references therein]. However, unlike the QD system, atomic Zeeman coherence does not necessarily involve two differentiable electrons, in contrast to the experiment we present here.

Finally, it is critical to note that while the simple discussion related to Fig. 1 shows the origin of the entanglement, the discussion is considerably over-simplified; it completely disregards the possibility that fast dephasing of the Zeeman coherence could lead to an unobservable effect, even if the single-exciton states themselves were long-lived. In the language of NMR, this is saying that a long T_1 and T_2 associated with the single-exciton states does not guarantee a comparable T_2 for the Zeeman coherence. The magnitude of the decoherence rate, γ_{ij} ($1/T_2$), in Eq. 2 can be determined by comparing the relative strength of the coherent and incoherent contribution. The dephasing rate of the radiative coherence was already shown in (*24*) to be ~20 ps and is comparable to the energy relaxation rate, Γ ($1/T_1$). This measurement further gives the decay rate of the Zeeman coherence as ~20 ps, which again is similar to the energy relaxation rate and shows that the pure dephasing of the two-exciton coherence is not significant in QDs. By exchanging the spectral position of the pump and the probe (the polarization has to be changed accordingly, too), the relative time scale of incoherent spin relaxation can also be estimated. As expected, the Zeeman splitting has reduced this process to an unobservable level (>100 ps).

In summary, we have inferred from our measurements entanglement of an excitonic system in single GaAs QDs and shown the importance of exciton-exciton Coulomb interaction for this observation. Our results are explained by a three-level model in a two-exciton basis. The next step, though more challenging, is to recover the same type of entanglement between coupled QDs [as proposed, for example, in (*13, 14*)]. This would allow for scaling the experiment to larger systems.

References and Notes

1. A. Einstein, B. Podolsky, N. Rosen, *Phys. Rev.* **47**, 777 (1935).
2. E. Schrödinger, *Proc. Camb. Philos. Soc.* **31**, 555 (1935).
3. R. J. C. Spreeuw, *Found. Phys.* **28**, 361 (1998).
4. For an introductory review, see the special issue on quantum information [*Phys. World* **11**, 33 (March 1998)].
5. See the review by A. Zeilinger [*Rev. Mod. Phys.* **71**, S288 (1999)] for discussions on entangling photons.
6. C. A. Sackett *et al.*, *Nature* **404**, 256 (2000).
7. Q. A. Turchette *et al.*, *Phys. Rev. Lett.* **81**, 3631 (1998).
8. E. Hagley *et al.*, *Phys. Rev. Lett.* **79**, 1 (1997).
9. See the article in the Search and Discovery section [*Phys. Today* **53**, 20 (January 2000)] for discussions on entanglement in liquid-state NMR. For experimental demonstrations of quantum algorithms using NMR, see, for example, I. L. Chuang *et al.*, *Phys. Rev. Lett.* **80**, 3408 (1998).
10. C. Monroe, D. M. Meekhof, B. E. King, W. M. Itano, D. J. Wineland, *Phys. Rev. Lett.* **75**, 4714 (1995).
11. Q. A. Turchette, C. J. Hood, W. Lange, H. Mabuchi, H. J. Kimble, *Phys. Rev. Lett.* **75**, 4710 (1995).
12. J. Ahn, T. C. Weinacht, P. H. Bucksbaum, *Science* **287**, 463 (2000).
13. A. Ekert and R. Jozsa, *Rev. Mod. Phys.* **68**, 733 (1996).
14. D. Loss and D. P. DiVincenzo, *Phys. Rev. A* **57**, 120 (1998).
15. A. Imamoglu *et al.*, *Phys. Rev. Lett.* **83**, 4204 (1999).
16. G. Schedelbeck, W. Wegscheider, M. Bichler, G. Abstreiter, *Science* **277**, 1792 (1997).
17. C. B. Murray, C. R. Kagan, M. G. Bawendi, *Science* **270**, 1335 (1995).
18. L. J. Sham and T. M. Rice, *Phys. Rev.* **144**, 708 (1966).
19. For two noninteracting systems under the excitation scheme described in the text, the total wavefunction is factorizable. This is explicit from the total Hamiltonian of the system, which is a sum of two independent Hamiltonians describing each system under excitation. The coupling needed for entanglement is provided through a number of ways under different circumstances. In cavity QED, the atoms are coupled through cavity fields. The Coulomb interaction provides the coupling for entangling two trapped ions and in our case, two excitonic transitions in a single quantum dot.
20. T. Östreich, K. Schönhammer, L. J. Sham, *Phys. Rev. Lett.* **75**, 2554 (1995).
21. See, for example, K. Bottet *et al.*, *Phys. Rev. B* **48**, 17418 (1993).
22. K. Brunner, G. Abstreiter, G. Böhn, G. Tränkle, G. Weimann, *Phys. Rev. Lett.* **73**, 1138 (1994).
23. In the case of entangling two trapped ions (*7*), one needs to rely on their common phonon modes that result from the Coulomb interaction. Since the ions are well separated in space, the weak interaction only creates collective motional modes without affecting their internal states. Therefore, none of the electronic states within one ion is mixed with those of its neighbor. Each level of the four-level model would in fact consist of a series of sublevels with the phonon modes incorporated. For some carefully arranged excitation (red-sideband excitation) and a specific initial condition (two-ion ground state with one phonon), no sublevels in the fourth (upper-most) level are resonant with the laser beams, resulting in a zero-probability amplitude of this level and therefore a nonfactorizable wavefunction.
24. N. H. Bonadeo *et al.*, *Phys. Rev. Lett.* **81**, 2759 (1998).
25. For our experiment, the pump and probe fields (E_{pump} and E_{probe}) are amplitude-modulated by two standing-wave acousto-optical modulators at frequency f_{pump} and f_{probe}, respectively. These frequencies (~100 MHz) are sufficient to suppress the slow nonelfectronic nonlinearities as well as the Overhauser effect present in the system. The third-order coherent nonlinear field $E_{NL}^{(3)}$ proportional to $\chi^{(3)} E_{pump} E^*_{pump} E_{probe}$ is emitted along the probe direction. A photodetector placed in the transmitted probe beam along with a lock-in amplifier phase-locked to $f_{pump} - f_{probe}$ detects signal that is proportional to the real part of $E^{(3)}_{NL} E^*_{probe}$ [the imaginary part of $\chi^{(3)}$]. The pump and the probe are from the same laser for the degenerate experiment and from two separate but mutually coherent lasers for the nondegenerate experiment.
26. D. Gammon, E. S. Snow, B. V. Shanabrook, D. S. Katzer, D. Park, *Phys. Rev. Lett.* **76**, 3005 (1996).
27. _____, *Science* **273**, 87 (1996).
28. S. W. Brown, T. A. Kennedy, D. Gammon, *Phys. Rev. B* **54**, R17339 (1996).
29. I. M. Beterov and V. P. Chebotaev, *Prog. Quantum Electron.* **3**, 1 (1974).
30. The mutual coherence bandwidth for the two lasers must be less than the decay rate of the coherence between the two excitons. The two lasers used in our measurement have a mutual bandwidth of about 3 MHz.
31. C. Sieh *et al.*, *Phys. Rev. Lett.* 82, 3112 (1999).
32. C. H. Bennett, D. P. DiVincenzo, J. A. Smolin, W. K. Wootters, *Phys. Rev. A* **54**, 3824 (1996).
33. K. Ferrio and D. Steel, *Phys. Rev. Lett.* **80**, 786 (1998).

34. This work was supported in part by the National Security Agency and Advanced Research and Development Activity under Army Research Office grant DAAG55-98-1-0373, Air Force Office of Scientific Research grant F49620-99-1-0045, NSF grant DMR 97-21444, and the Office of Naval Research. We thank R. Merlin, P. Berman, H. J. Kimble, D. Wineland, and D. DiVincenzo for helpful discussions, and R. Merlin for loaning critical equipment.

29 March 2000; accepted 4 August 2000

Evidence That the Reactivity of the Martian Soil Is Due to Superoxide Ions

A. S. Yen,[1]* S. S. Kim,[1] M. H. Hecht,[1] M. S. Frant,[2] B. Murray[3]

The Viking Landers were unable to detect evidence of life on Mars but, instead, found a chemically reactive soil capable of decomposing organic molecules. This reactivity was attributed to the presence of one or more as-yet-unidentified inorganic superoxides or peroxides in the martian soil. Using electron paramagnetic resonance spectroscopy, we show that superoxide radical ions (O_2^-) form directly on Mars-analog mineral surfaces exposed to ultraviolet radiation under a simulated martian atmosphere. These oxygen radicals can explain the reactive nature of the soil and the apparent absence of organic material at the martian surface.

The 1976 Mars Viking Landers performed a series of experiments in which soil samples were analyzed for evidence of life. Biological responses were not detected; however, the soil samples from the surface as well as from ~10 cm beneath the immediate surface were found to be chemically reactive (*1*). Upon the introduction of water vapor, oxygen was released from the soil samples in larger quantities than would be expected from physical adsorption in equilibrium with the ambient atmosphere (*2*). Furthermore, isotopically la-